

Near-Edge X-ray Absorption Fine Structure Spectroscopy on Ordered Films of an Amphiphilic Derivate of 2,5-Diphenyl-1,3,4-Oxadiazole

R. Giebler,^{†,||} B. Schulz,[†] J. Reiche,[†] L. Brehmer,[†] M. Wühn,[‡] Ch. Wöll,[‡]
A. P. Smith,[§] S. G. Urquhart,[§] H. W. Ade,[§] and W. E. S. Unger^{*,||}

Universität Potsdam, Lehrstuhl für Physik der kondensierten Materie, Postfach 601553,
D-14415 Potsdam, Germany, Ruhr-Universität Bochum, Lehrstuhl für Physikalische Chemie I,
D-44780 Bochum, Germany, Physics Department, North Carolina State University, Box 8202,
Raleigh, North Carolina 27695, and Bundesanstalt für Materialforschung und -prüfung,
Lab. VIII.23, Unter den Eichen 44-46, D-12203 Berlin, Germany

Received July 14, 1998. In Final Form: November 19, 1998

The surfaces of ordered films formed from an amphiphilic derivative of 2,5-diphenyl-1,3,4-oxadiazole by the Langmuir–Blodgett (LB) technique and organic molecular beam deposition (OMBD) were investigated by the use of near-edge X-ray absorption fine structure (NEXAFS) spectroscopy. For the assignment of the spectral features of the C, N, and O K-edge absorption spectra, fingerprint spectra of poly(*p*-phenylene terephthalamide) (Kevlar), poly(ethylene terephthalate), poly(*p*-phenylene-1,3,4-oxadiazole), and 2,5-di-(pentadecyl)-1,3,4-oxadiazole, which contain related chemical moieties, were recorded. Ab initio molecular orbital calculations, performed with explicit treatment of the core hole, are used to support the spectral interpretations. Angle-resolved NEXAFS spectroscopy at the C, N, and O K-edges suggests a preferentially upright orientation of the oxadiazole derivative in the outermost layer of the films. X-ray specular reflectivity data and molecular modeling results suggest a similar interpretation.

Introduction

The formation of highly ordered films of organic molecules is a challenging way to obtain materials with unique physical properties. Organic materials containing the oxadiazole unit are of great interest, as they are thermally stable and have interesting electro-optical and electronic properties.¹ The application of oxadiazoles in electroluminescence devices is a strong motivation for the fundamental investigation of this class of substances. Schulz et al. described the use of aromatic poly(1,3,4-oxadiazole)s as the light-emitting material in a single-layer LED.² In such devices the interface between the active organic layer and the metallic electrodes plays an essential role, as the electric charge carriers have to pass through it. The kind of chemical interaction between both materials is important for the efficiency of the device, as it influences the electronic structure and the charge transport at the interface.³

Near-edge X-ray absorption fine structure (NEXAFS) spectroscopy is known to be a powerful tool for investigating the surface of organic materials and their alteration by plasma treatment, metallization, and so forth.⁴ In this contribution we present NEXAFS spectra of the surface of an organic model system consisting of oxadiazole molecules which, in further investigations, shall be used for the formation of interfaces to different metals.

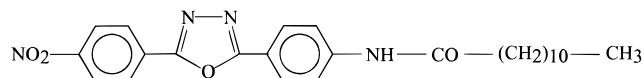


Figure 1. Amphiphilically substituted 2,5-diphenyl-1,3,4-oxadiazole AF51 used for film preparation by the LB technique and by OMBD.

A NEXAFS spectrum is recorded by scanning the incident photon energy across an absorption edge and measuring the absorption of photons by the sample.⁵ This absorption can be measured through the emission of secondary electrons (partial or total electron yield), the emission of fluorescent photons (fluorescent yield), or the transmission of X-rays through the sample. Peaks appear at photon energies that correspond to electronic transitions from core levels to unoccupied molecular orbitals in a molecule or polymer. When measured by partial electron yield, NEXAFS spectroscopy has a high surface sensitivity.

Experimental Section

Materials, Film Preparation, and Characterization. The Langmuir–Blodgett (LB) technique and organic molecular beam deposition (OMBD) were applied to prepare ordered organic films with typical thicknesses of about 30–60 nm on silicon substrates. Details of the film preparation and their characterization by X-ray reflectometry and scanning force microscopy (SFM) as well as details of molecular modeling calculations are described elsewhere.^{6–8} An amphiphilically substituted 2,5-diphenyl-1,3,4-

* Author for communication. Telephone: ++49 30 8104 1823. Fax: ++49 30 8104 1827. E-mail: Wolfgang.Unger@bam.de.

[†] Universität Potsdam.

[‡] Ruhr-Universität Bochum.

[§] North Carolina State University.

^{||} Bundesanstalt für Materialforschung und -prüfung.

(1) Schulz, B.; Bruma, M.; Brehmer, L. *Adv. Mater.* **1997**, 9 (8), 601.

(2) Schulz, B.; Kaminor, Y.; Brehmer, L. *Synth. Met.* **1997**, 84, 449.

(3) Bigerson, J.; Fahlmann, M.; Bröms, P.; Salaneck, W. R. *Synth. Met.* **1996**, 80, 125.

(4) Unger, W.; Lippitz, A.; Wöll, Ch.; Heckmann, W. *Fresenius J. Anal. Chem.* **1997**, 358, 89.

(5) Stöhr, J. *NEXAFS Spectroscopy*; Springer Series in Surface Science 25; Springer: New York, 1992.

(6) Reiche, J.; Schulz, B.; Knochenhauer, G.; Dietzel, B.; Freydank, A.; Zetzsche, T.; Brehmer, L. *Thin Solid Films* **1997**, 295, 241.

(7) Reiche, J.; Knochenhauer, G.; Dietel, R.; Freydank, A.; Zetzsche, T.; Geue, T.; Barberka, T. A.; Pietsch, U.; Brehmer, L. *Supramol. Sci.* **1997**, 4, 455.

(8) Reiche, J.; Freydank, A.; Helms, A.; Stiller, B.; Knochenhauer, G.; Schulz, B.; Brehmer, L. In *Proceedings of the Seventh European Conference on Thin Organised Films (ECOF-7)*, Sept. 14–18, 1998, Potsdam, Germany; University of Potsdam: Potsdam, Germany; pp 257–58.

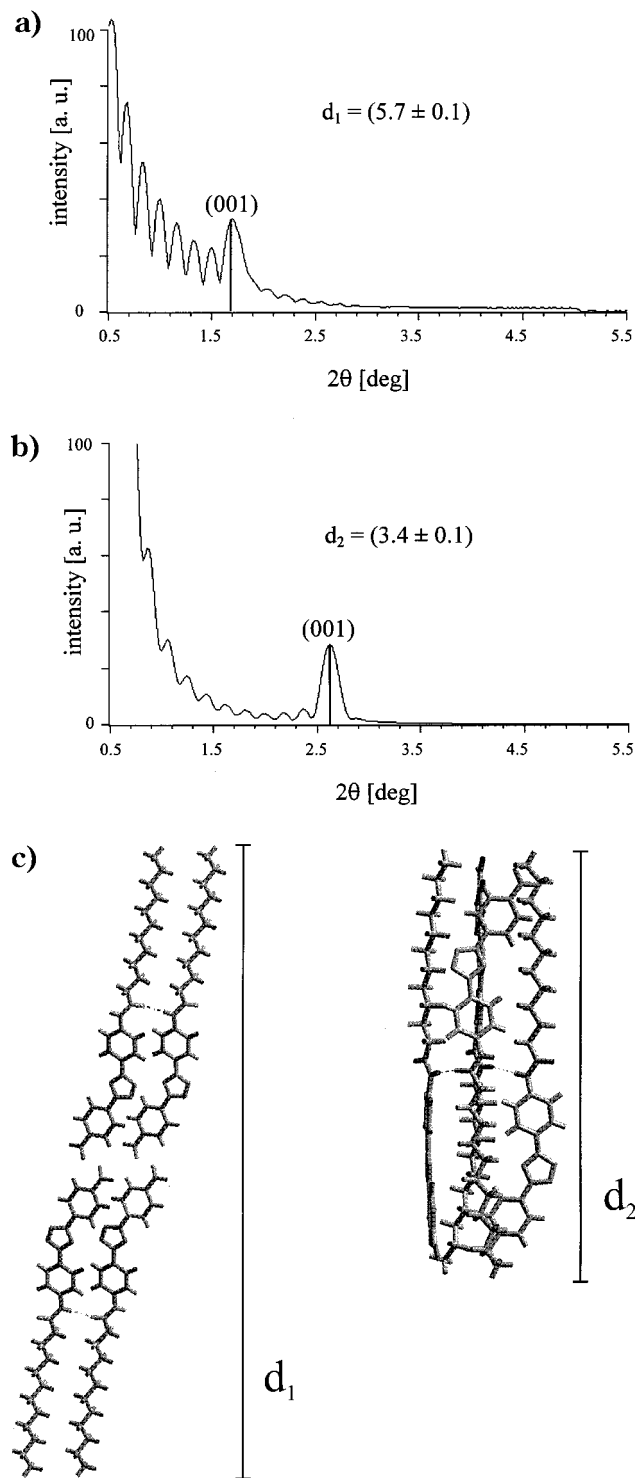


Figure 2. (a) X-ray reflectivity data of an oxadiazole AF51 LB film. (b) X-ray reflectivity data of an OMBD film of AF51. (c) Structure models for the LB and OMBD films derived from molecular modeling with $d_1 = 5.7$ and $d_2 = 3.3$ nm.

oxadiazole (AF51), whose structure is shown in Figure 1, was used for the film preparation. The substituents in this molecule were inserted in order to guarantee good film formation and stabilization properties for the LB technique.⁷

Kiessig fringes, which appear in the X-ray specular reflection curves of both LB and OMBD films (Figure 2a and b), allow the calculation of the total film thickness and indicate a rather smooth surface. The latter fact is also confirmed by SFM data, which yield a value of about 0.4 nm root mean square roughness. The bilayer thickness of the LB multilayers, following from the position of the (001) peak in the X-ray reflectivity curve, is $d =$

(5.7 ± 0.1) nm. Obviously, the molecules do not form the same bilayer structure in the case of the OMBD films. The observed layer spacing of $d = (3.4 \pm 0.1)$ nm is different from that of the virgin LB films. The layer spacing is, however, very close to that of LB films thermally cured at about 100 °C.⁷ Molecular modeling simulations based on these experimental data allow us to establish a hypothesis for the molecular structure of LB and OMBD films. The results suggest a preferentially upright orientation of the oxadiazole molecules relative to the surface plane for both the LB and OMBD films (see Figure 2c). The layer spacings, 5.7 and 3.3 nm, respectively, obtained by molecular modeling are a result of the different arrangements of the oxadiazole molecules in LB and OMBD films.

Samples of poly(*p*-phenylene terephthalamide) (Kevlar), poly(ethylene terephthalate) (PET), poly(*p*-phenylene-1,3,4-oxadiazole) (PPOD), and 2,5-di(pentadecyl)-1,3,4-oxadiazole (DPOD) were used for the recording of fingerprint spectra. The PET sample is a commercially available biaxially stretched 0.5 μ m PET foil (Mylar, Du Pont de Nemours). The PPOD and DPOD samples were prepared as spin-coated films on silicon substrates at the *Institut für Dünnschichttechnologie und Mikrosensorik (IDM)*, Teltow, Germany.

X-ray Absorption Spectroscopy. The spectra of Kevlar were measured at beamline X1A at the National Synchrotron Light Source (NSLS) in Brookhaven, NY.⁹ The NEXAFS analysis of all other samples was performed at HE-TGM2 beamline #33.12 of the synchrotron light source BESSY (Berlin, Germany). The features of this toroidal grating monochromator are given in BESSY's users' handbook (Jung, Ch., Ed.; Berlin, 1993). Second-order contributions (around 5%) were not crucial for the described experiments. The spectra were recorded at the C 1s, N 1s, and O 1s absorption K-edges in the partial electron yield (PEY) detection mode with a retarding voltage of -150 V. The resolution at the C 1s edge was always better than 0.7 eV. The information depth (95%) of the NEXAFS method in the PEY mode can be estimated to be ≤ 30 Å for the C signal, ≤ 40 Å for the N signal, and ≤ 50 Å for the O signal.¹⁰ Low-energy electrons that mostly originate from deeper layers were suppressed by the preset threshold energy from entering the detector. The energy scale of the C K-edge spectra was calibrated by setting the C 1s $\rightarrow \pi^*$ resonance of a highly oriented pyrolytic graphite (HOPG) reference film (Advanced Ceramic Corp., Cleveland, OH) to 285.38 eV.¹¹ For the energy scale calibration of the O K-edge spectra, the O 1s $\rightarrow \pi^*_{C=O}$ resonance of a poly(ethylene terephthalate) (PET) sample was set to 531.5 eV. Urquhart et al., using calibrated inner shell electron energy loss spectra (ISEELS), determined this value.¹² Characteristic features in the incident flux monitor signals were used to align the energy scales of all spectra relative to these values. The energy scale of the N K-edge spectra, which for all samples were recorded immediately after monitoring the C K-edges, was calibrated by using the same energy offset which was determined for the characteristic features in the flux monitor signals of the C K-edge spectra measured before.

After energy calibration, the spectra were corrected for the monochromator transmission by dividing them by the NEXAFS spectra of a clean gold sample. Subsequently they were normalized to the absorption jumps at 325, 435, and 575 eV, respectively, a procedure proposed elsewhere.⁵ The reproducibility of the spectra was carefully checked by multiple scanning. No indication of beam damage effects was found.

To look for orientations of the molecules in the films, NEXAFS spectra were recorded at nominal angles of 30°, 55°, and 90° by rotating the sample about a vertical axis. These angles are defined to be measured between the surface plane of the sample and the direction vector of the synchrotron light beam. The inset in Figure 9 illustrates the geometry of the experiment. The light is linearly polarized. An angle of 90° means normal incidence of the light; that is, the electric field vector **E** lies in the surface plane of the organic film. 30° means grazing incidence of light; that is, **E** is preferentially parallel to the surface normal of the film.

(9) Ade, H.; Smith, A. P.; Zhang, H.; Zhuang, G. R.; Kirz, J.; Rightor, E.; Hitchcock, A. *J. Electron Spectrosc. Relat. Phenom.* **1997**, *84*, 53.

(10) Seah, M. P.; Dench, W. A. *Surf. Interface Anal.* **1979**, *1*, 2.

(11) Batson, P. E. *Phys. Rev. B* **1993**, *48*, 2608.

(12) Urquhart, S. G.; Hitchcock, A. P.; Smith, A. P.; Ade, H.; Rightor, E. G. *J. Phys. Chem.* **1997**, *101*, 2267.

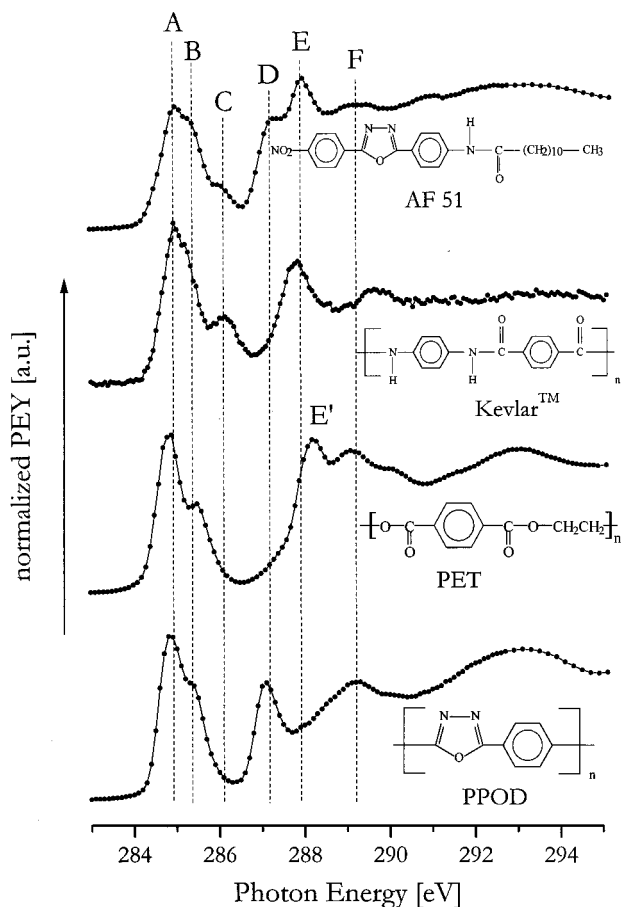


Figure 3. C K-edge X-ray absorption spectra of AF51, Kevlar, PET, and PPOD for fingerprinting. The interpretation of the spectral features marked by capitals is given in the text and in Table 1.

Theoretical Calculations. Calculations of the C 1s and N 1s core excitation spectra of poly(*p*-phenylene-1,3,4-oxadiazole) (PPOD) and 2,5-di(phenadecyl)-1,3,4-oxadiazole (DPOD) were performed using Kosugi's GSCF3 program.¹³ In this program, the effect of the core hole on the electronic structure is incorporated through the *Improved Virtual Orbital* approximation.¹⁴ This relaxed Hartree–Fock potential is essential for accurately considering the large electronic reorganization upon inner shell hole creation and is superior to using ground-state orbitals. This method has been applied successfully to calculations of the core excitation spectra of poly(ethylene terephthalate) and isomerically related polyphthalates,¹² organosilanes,¹⁵ and carboranes.¹⁶ This method also calculates the ionization potential through the energy difference between the ground-state and core-ionized-state calculations (ΔSCF).

The model structures **1a** and **2a** (shown in Figure 4a) are considered for models for the phenyl and oxadiazole environments, respectively, in PPOD. In both cases, the functional group of interest (phenyl or oxadiazole) is substituted by the adjacent functional group (oxadiazole or phenyl, respectively). These models are chosen to reproduce the electronic delocalization between the phenyl and oxadiazole groups while still being small enough for high-quality *ab initio* calculations. The possibility that longer range electronic delocalization has an effect on the core excitation spectrum is evaluated by smaller basis set calculations of model **1a** and models incorporating several repeat units: **1b** and **1c** (see model schemes in Figure 4a). Structure

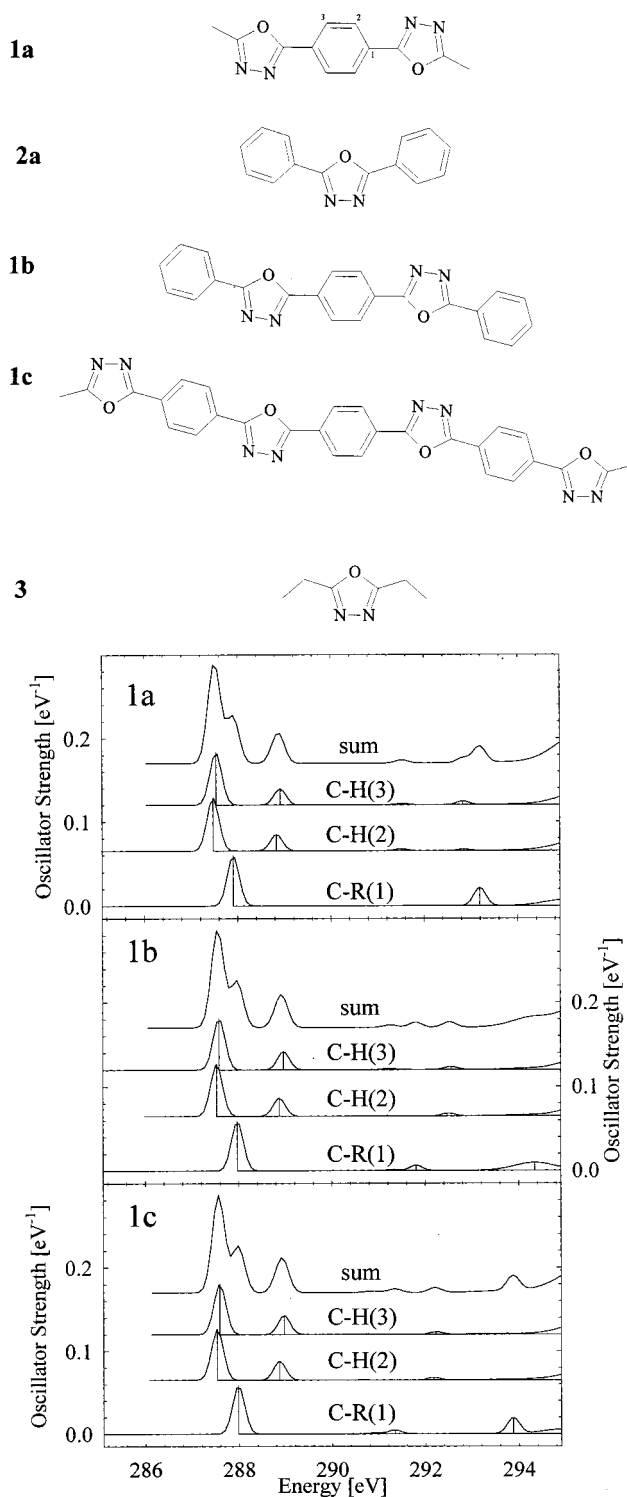


Figure 4. (a, top) Schemes of models used for the quantum chemical calculations. (b, bottom) Comparison of the *ab initio* calculated C 1s core excitation spectra of the symmetry inequivalent carbons in the central phenyl group in models **1a**, **1b**, and **1c**. Each component spectrum corresponds to an IVO calculation for a specific site. The excitation energy is the sum of the calculated term value for individual transitions and the calculated IP. The peak areas are calculated absolute oscillator strengths, and the sum is weighted by stoichiometry.

3 is used as a model for the oxadiazole environment in DPOD. The replacement of the pentadecyl group by an ethyl group is not expected to have an effect of the spectrum of the unsaturated oxadiazole group.

Geometries for structures **1a**, **2a**, and **3** were obtained by geometry optimization at the 6-31G* level using the program

(13) Kosugi, N.; Kuroda, H. *Chem. Phys. Lett.* **1980**, *74*, 490.

(14) Hunt, W. J.; Goddard, W. A. *Chem. Phys. Lett.* **1968**, *3*, 414.

(15) Urquhart, S. G.; Turci, C. C.; Tylliszczak, T.; Brook, M. A.; Hitchcock, A. P. *Organometallics* **1997**, *16*, 2080.

(16) Hitchcock, A. P.; Urquhart, S. G.; Wen, A. T.; Kilcoyne, A. L. D.; Tylliszczak, T.; Rühl, E.; Kosugi, N.; Bozek, J. D.; Spencer, J. T.; McIlroy, D. N.; Dowben, P. A. *J. Phys. Chem.* **1997**, *101*, 3483.

GAMESS.¹⁷ The calculated bond lengths for **1a** and **2a** correspond to trends presented from the AM1 and density functional calculations of Brocks and Tol.¹⁸ The structures of models **1b** and **1c** were constructed using the calculated geometries of the smaller models **1a** and **2a**.

For the GSCF3 calculations, the basis set used is that of Huzinaga et al.¹⁹ For the PPOD model, two series of calculations were performed: a modest basis set study of models **1a**, **1b**, and **1c** and a higher quality calculation of models **1a** and **2a**. For the first study, (43/4) contracted Gaussian type functions were used on the heavy atoms (C, N, and O), (4) was used on H, and a slightly higher quality basis set (31121/3111) was used on the heavy atom onto which the core hole is placed. In the higher quality calculations performed on models **1a** and **2a**, the following basis sets are employed: (621/41) contracted Gaussian type functions on the heavy atoms (C, N, and O); (41) on H; and a higher quality basis set (411121/3111/*) on the heavy atom onto which the core hole is placed. These basis sets were also used for the calculation performed on model **3**. In all cases, a separate calculation is performed for each symmetry inequivalent core excited atom of interest.

Simulated spectra are generated from the computational results using a Gaussian line shape for each calculated excitation. The width of these Gaussians is 0.3 eV for orbitals of eigenvalue (e) $-15 < \epsilon < 0$, 1.2 eV for $0 < \epsilon < 4$ in the C 1s simulation, and 0.6 eV for orbitals of eigenvalue (e) $-15 < \epsilon < 0$ for the O 1s and N 1s simulations. These widths are chosen to be similar to the experimentally observed line widths. The simulated spectra are set to experimental scale by setting the zero of the calculated term value scale ($\epsilon = 0$) to the calculated (Δ SCF) ionization potential.

Results and Discussion

Interpretation of Spectral Features. An empirical, somewhat "enlarged" building block approach can be used to interpret the spectra of larger molecules such as AF51. In the original approach proposed by Stöhr,⁵ the spectra of large systems can be viewed as an assembly of "diatomic" or "pseudo-diatomic" building block contributions. As both Stöhr⁵ and other authors²⁰ have noted, electronic delocalization and conjugation limit the "pseudo-diatomic" building block approach. For such complex systems, larger building blocks are useful, such as those based on the functional groups present in the larger molecule or polymer^{12,21–24} or a series of polymer repeat units.²⁰ In general, *empirical comparisons* work for understanding the spectra of complex polymers and models. Comparisons of the fingerprint spectra of polymers and molecules with similar chemical environments to that of the polymer of interest are useful and are the basis for this study.

The successful application of the building block approach for the spectrum of PET was attributed to the absence of electronic interactions between the building block groups.^{12,22} In PET, a saturated ethyl linkage separates the aromatic segments in the PET chain, decreasing the π electronic interaction between the repeat units. In

Table 1. Assignment of the Resonant Features for the C K-Edge NEXAFS Spectra of the Oxadiazole Molecule AF51

resonance	energy (eV)	assignment
A	285.0	$\pi^*_{C=C}$, phenyl
B	285.3	$\pi^*_{C=C}$, phenyl
C	286.1	$\pi^*_{C=C}$, phenyl, NO ₂ or NH ligand related
D	287.3	$\pi^*_{C=N}$, oxadiazole
E	288.0	$\pi^*_{C=O}$, carbonyl

polymers with an entirely aromatic backbone, such as PPOD, a simple functional-group-based building block interpretation must be approached with caution, as extensive electronic delocalization along the polymer chain is expected to significantly perturb the electronic spectra.

To provide an empirical basis for the spectral interpretation of PPOD, spectra of substances that contain similar moieties, such as DPOD, PET, PPOD, Kevlar, and others, were recorded. Published NEXAFS spectra of benzene,⁵ nitrobenzene,²⁵ aniline,²⁵ and oxazole²⁶ were included in the interpretation. In addition, calculations of the C 1s and N 1s core excitation spectra of poly(*p*-phenylene-1,3,4-oxadiazole) (PPOD) were performed. This was done in order to elucidate the contribution of the 2,5-diphenyl-1,3,4-oxadiazole unit to the C K-edge and N K-edge NEXAFS spectra of AF51.

All fingerprint spectra were measured at the magic incidence angle $\theta \approx 55^\circ$, as for this incidence angle the measured intensity distribution is independent of the molecular orientation.⁵ The NEXAFS spectra of the oxadiazole molecule AF51 shown in Figures 3, 6, and 8 were recorded from an OMBD film. Spectra of a LB film, not shown here, were also recorded. As is expected, they show the same spectral features and nearly coincide with the spectra of the OMBD film.

C K-Edge Spectra: Experiment. The C K-edge absorption spectra were measured at photon energies between 280 and 330 eV. However, in Figure 3 only the energy range between 283 and 295 eV is shown. Energies and assignments are listed in Table 1. By comparing the C K-edge spectrum of AF51 with those of Kevlar, PET, and PPOD, the following assignments can be made:

As all four substances contain phenyl rings, their spectra are dominated by a sharp C 1s(C–H) $\rightarrow \pi^*_{C=C}$ (A) resonance near 285.0 eV. (The core level is indicated parenthetically before the arrow, while the nature of the upper level of a given transition is indicated by the final subscript.) This feature is accompanied by a shoulder (B) at 285.3 eV. The peak (C) at 286.1 eV is a C 1s(C–R) $\rightarrow \pi^*_{C=C}$ component of resonance A. Peak C should be due to core excitations from the "C–R" phenyl carbon that is attached to the N ligands, that is, to amide and nitro groups.^{5,9} The inductive effect of the amine group shifts the C 1s ionization potential of the C–R phenyl carbon to lower energy, increasing the energy of the C 1s(C–R) $\rightarrow \pi^*_{C=C}$ transition to the common manifold of π^* (LUMO) states. This resonance (C) is only present in the polymers where the phenyl group is attached to an N ligand (AF51 and Kevlar) but not in PET and PPOD. Calculations of PET¹² and PPOD (this communication) support this assignment.

The feature (D) at 287.3 eV is assigned to a C 1s $\rightarrow \pi^*_{C=N}$ resonance of the oxadiazole ring. It is only present in the spectra of AF51 and PPOD, and its π character is

(17) Schmidt, M. W.; Baldrige, K. K.; Boatz, J. A.; Elbert, S. T.; Gordon, M. S.; Jensen, J. H.; Koseki, S.; Matsunaga, N.; Nguyen, K. A.; Su, S. J.; Windus, T. L.; Dupuis, M.; Montgomery, J. A. *J. Comput. Chem.* **1993**, *14*, 1347.

(18) Brocks, G.; Tol, A. *J. Chem. Phys.* **1997**, *106* (15), 6418.

(19) Huzinaga, S.; Andzelm, J.; Klobukowski, M.; Radzio-Andzelm, E.; Sasaki, Y.; Tatewaki, H. *Gaussian Basis Sets for Molecular Calculations*; Elsevier: Amsterdam, 1984.

(20) Carravetta, V.; Ågren, H.; Pettersson, L. G. M.; Vahtras, O. *J. Chem. Phys.* **1995**, *102*, 5589.

(21) Hitchcock, A. P.; Urquhart, S. G.; Rightor, E. G. *J. Phys. Chem.* **1992**, *96*, 8736.

(22) Urquhart, S. G.; Hitchcock, A. P.; Leapman, R. D.; Priester, R. D.; Rightor, E. G. *J. Polym. Sci., Part B: Polym. Phys.* **1995**, *33*, 1593.

(23) Urquhart, S. G. Ph.D. Thesis, McMaster University (Hamilton, ON), 1997.

(24) Pettersson, L. G. M.; Ågren, H.; Schürmann, B. L.; Lippitz, A.; Unger, W. E. S. *Int. J. Quantum Chem.* **1997**, *64*, 749.

(25) Turci, C.; Urquhart, S.; Hitchcock, A. *Can. J. Chem.* **1996**, *74*, 851.

(26) Hennig, C.; Hallmeier, K. H.; Bach, A.; Bender, S.; Franke, R.; Hormes, J.; Szargan, R. *Spectrochim. Acta, Part A* **1996**, *52*, 1079.

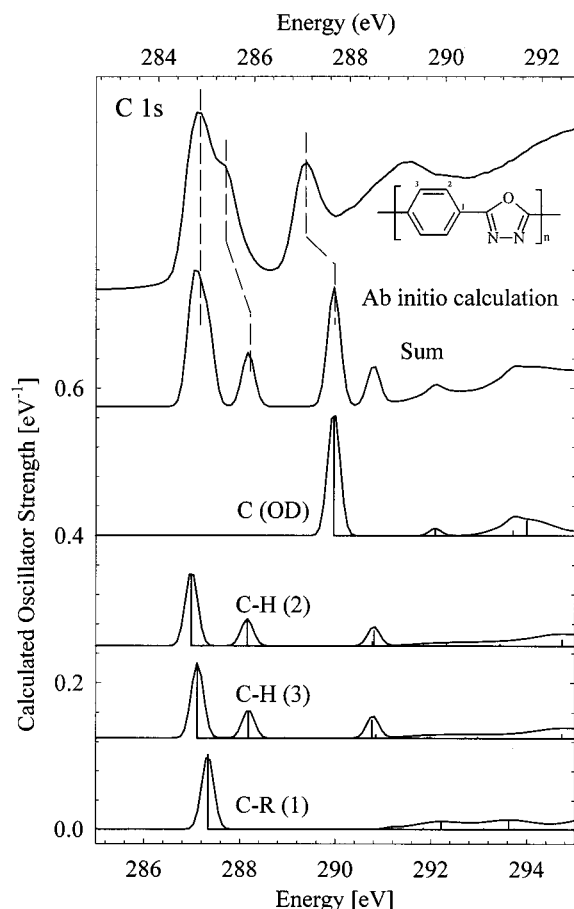


Figure 5. Comparison of the high-quality ab initio calculation of models **1a** and **2a** with the experimental C K-edge NEXAFS spectrum of PPOD. The energy scales of the calculation and the experiment are offset by 2.3 eV in order to align the energy of the lowest C 1s $\rightarrow \pi^*$ transition (see caption of Figure 4 for additional computational details).

clearly proved by its angle dependence shown in Figure 9, which corresponds to the angular dependence of the π^* phenyl resonances. Unfortunately, the C K-edge spectrum of DPOD, which was the only available material containing the pure oxadiazole unit without any further π systems at this time, is dominated by the resonances of its alkyl substituents. Its spectrum resembles the C K-edge spectrum of PP or PE^{4,9} and is therefore not shown in Figure 3.

The resonance (E) at 288.0 eV is assigned to a C 1s $\rightarrow \pi^*_{C=O}$ excitation. This feature appears near the same energy for AF51, PET, and Kevlar. It is not too surprising that the carbonyl-specific signals for PET and Kevlar differ slightly in energy from that for AF51, as these carbonyl groups are in slightly different chemical environments. Similar shifts in the carbonyl C 1s $\rightarrow \pi^*_{C=O}$ transition energy have been observed before.^{22,27}

The features above 290 eV are covering broad σ^* resonance contributions attributed to ring, CH₂CH₂ sequence, C–O, C–N, C=O, and C=N bonds.

C K-Edge Spectra: Calculations. Figure 4b presents a comparative study of the C 1s core excitation spectrum of the central phenyl group in models **1a**, **1b**, and **1c**. The two C–H components and the C–R component represent the three symmetry inequivalent sites of the central phenyl group in each model. The spectra of this phenyl group in

Table 2. Calculated Energies, Term Values, Oscillator Strengths, and Ionization Potentials for the C 1s $\rightarrow \pi^*$ Transitions of PPOD Models **1a** and **2a**

	energy (eV)	term value (eV)	oscillator strength	assignment
1a; C–R (1); Ionization Potential = 291.59 eV				
1	287.34	4.26	0.0163	$1\pi^*_{C=C}$
2	289.42	2.18	0.0000	silent $\pi^*_{C=C}$
3	291.19	0.40	0.0003	π^*
1a; C–H (2); Ionization Potential = 290.99 eV				
1	286.99	4.00	0.0164	$1\pi^*_{C=C}$
2	288.16	2.83	0.0059	$1\pi^*_{C=C}$
3	290.77	0.22	0.0009	$\pi^*_{C=C}$
4	290.81	0.18	0.0033	3s Ryd?
1a; C–H (3); Ionization Potential = 291.06 eV				
1	287.12	3.94	0.0163	$1\pi^*_{C=C}$
2	288.19	2.87	0.0062	$1\pi^*_{C=C}$
3	290.77	0.29	0.0041	$\pi^*_{C=C}$
4	290.85	0.21	0.0008	3s Ryd?
2a; C-Oxadiazole; ionization potential = 293.89 eV				
1	289.96	3.92	0.0271	$\pi^*_{C=N}$
2	292.08	1.80	0.0016	π^*
3	293.31	0.58	0.0001	π^*
4	293.71	0.18	0.0011	π^*

the three models are nearly identical. This indicates that longer range electronic delocalization does not significantly perturb the core excitation spectrum of the oxadiazole group in this polymer and that the simple model **1a** is adequate to reproduce the extent of electronic delocalization in this polymer. This result supports our use of a building block approach in PPOD.

Figure 5 presents the results on the higher quality ab initio calculation of models **1a** and **2a**, in comparison to the experimental C 1s NEXAFS spectrum of PPOD. The energy scales of the calculation and the experiment are offset by 2.3 eV in order to align the energy of the lowest C 1s $\rightarrow \pi^*$ transition. The contributions from the three symmetry inequivalent phenyl carbons in model **1a** (position numbers indicated in the respective scheme in Figure 4a) and the one symmetry equivalent carbon site in the oxadiazole ring in model **2a** are presented. There are very slight differences between this calculation of model **1a** and the lower quality calculation of **1a** (see Figure 4b), but these are expected to arise from the poorer quality of the ionization potential calculation with the less flexible basis set. There is an excellent correspondence between the experimental and calculated features. The calculated ionization potentials, energies, term values, and oscillator strengths are presented in Table 2.

These calculations predict that the first peak in the C 1s spectrum corresponds to the C 1s $\rightarrow 1\pi^*_{C=C}$ transition, with nearly superimposed contributions for both the C–H and C–R phenyl ring carbon atoms. The origin of the second transition in the C 1s spectrum is of particular interest. This second π^* level is the higher energy partner of the degenerate e_{2u} π^* LUMO level in benzene, where the degeneracy is lifted by the reduction in molecular symmetry. This second π^* level is silent in benzene and most substituted phenyl species but has been previously observed and assigned in the C 1s spectrum of poly(ethylene terephthalate).¹² A discussion of the unique nature of this conjugative mixing in para-substituted-phenyl-containing polymers is in preparation.²⁸

At higher energy, the C 1s(OD) $\rightarrow \pi^*_{C=N}$ transition originating in the oxadiazole ring carbon occurs at 287 eV.

N K-Edge. The N K-edge absorption spectra were measured at photon energies between 395 and 435 eV,

(27) Urquhart, S. G.; Hitchcock, A. P.; Priester, R. D.; Rightor, E. G. *J. Polym. Sci., Part B: Polym. Phys.* **1995**, *33*, 1603.

(28) Urquhart, S. G.; Ade, H. W. Manuscript in preparation.

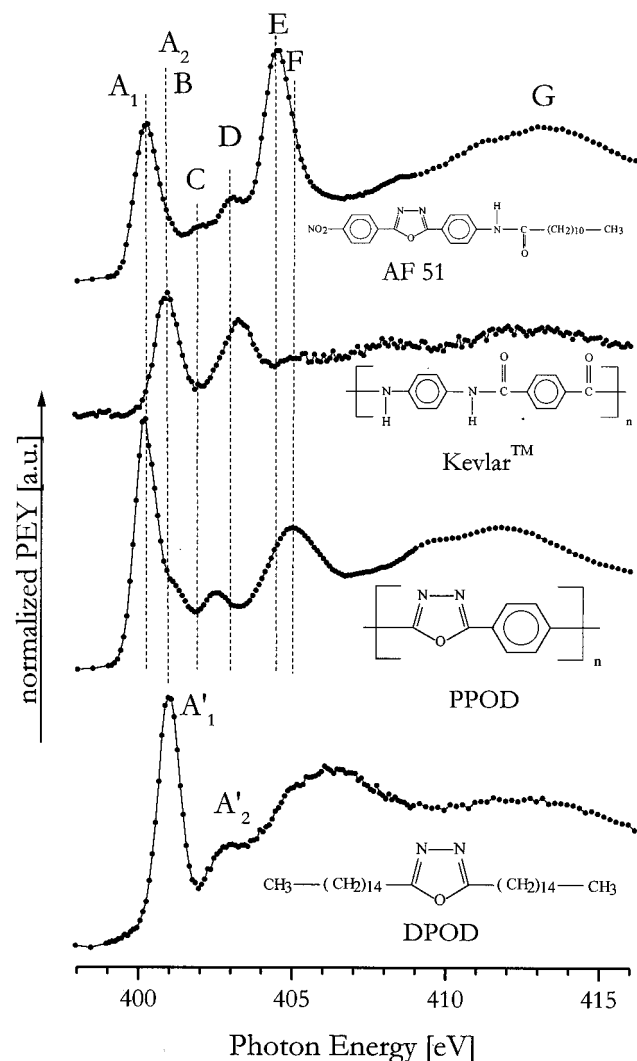


Figure 6. N K-edge X-ray absorption spectra of AF51, Kevlar, PPOD, and DPOD for fingerprinting. The interpretation of the spectral features marked by capitals is given in the text and in Table 3.

Table 3. Assignment of the Resonant Features of the N K-Edge NEXAFS Spectra of the Oxadiazole Molecule AF51

resonance	energy (eV)	oxadiazole	amine	NO ₂
A ₁	400.0	$\pi^*_{C=N}$		
A ₂ , B ₁	400.9	$\pi^*_{C=N}$	π^*_{N-Ph}	
C	402.5	σ^*_{N-N}		
D	403.2		σ^*_{N-H}	
E	404.5			$\pi^*_{N=O}$
F	405	σ^*_{N-R}		
G	413		σ^*_{N-R}	

but only the energy range between 398 and 416 eV is shown in Figure 6 to facilitate a better assignment of the π^* resonances. The energies and assignments of AF51 are presented in Table 3.

Resonance A₁ at 400.0 eV is assigned to the N 1s \rightarrow $p^*_{C=N}$ transition of the oxadiazole ring. It lies exactly at the same energetic position for AF51 and PPOD. Its π character is clearly proved by its angular dependence, which corresponds to the angular dependence of the C1s \rightarrow $\pi^*_{C=C}$ resonance of the phenyl ring and is shown in the N K-edge spectra of AF51 (Figure 9). The oxadiazole ring resonance (A₁) is accompanied by a second π^* resonance (A₂) at 401.2 eV in the spectrum of PPOD. In DPOD, these π^* resonances (A₁) and (A₂) are shifted by 1 eV to higher

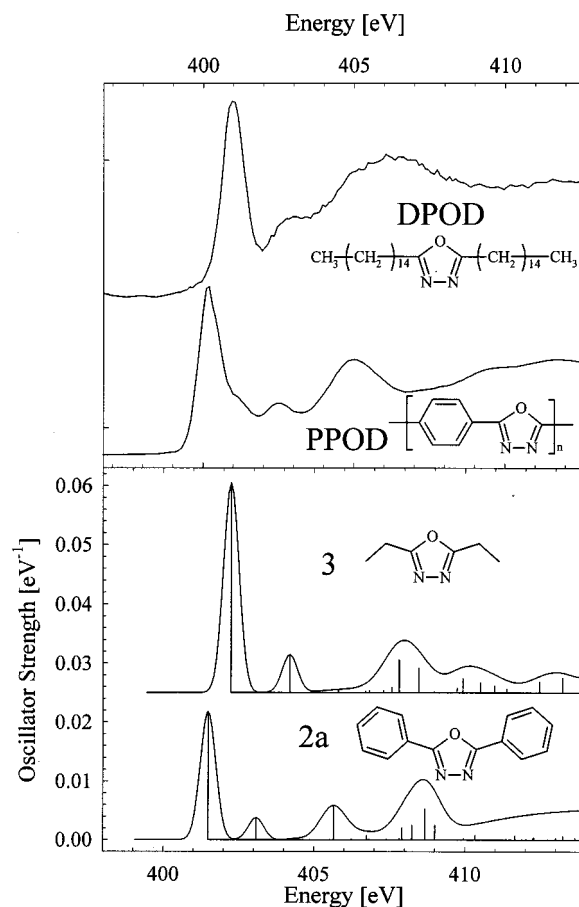


Figure 7. Calculated N 1s spectrum of models 2a and 3, in comparison to the experimental C K-edge NEXAFS spectra of PPOD and DPOD.

Table 4. Calculated Energies, Term Values, Oscillator Strengths, and Ionization Potentials for the N 1s \rightarrow π^* Transitions of PPOD Models 2a and 3

energy (eV)	term value (eV)	oscillator strength	assignment
Oxadiazole Model 2a; Ionization Potential = 405.07 eV			
1 401.49	3.58	0.0139	$\pi^*_{C=N}$
2 403.08	2.00	0.0024	π^*
3 404.38	0.69	0.0001	π^*
Dialkylloxadiazole Model 3; Ionization Potential = 405.45 eV			
1 402.25	3.21	0.0227	$\pi^*_{C=N}$
2 404.20	1.26	0.0041	π^*
3 405.13	0.33	0.0001	σ^*
4 405.79	-0.35	0.0006	σ^*

energy and have a wider splitting of ~ 2.5 eV. This splitting and energy correspond to N K-edge NEXAFS investigations by Hennig et al. on oxazole and other heterocycles.²⁶

Figure 7 presents the results of an ab initio calculation of the N K-edge spectra of the PPOD model 2a and the DPOD model 3, in comparison to the experimental N K-edge spectra of PPOD and DPOD. The calculated ionization potentials, energies, term values, and oscillator strengths are presented in Table 4. There is good correspondence between the experimental and calculated spectra of PPOD and DPOD, most markedly for the shift between the spectra of the phenyl and alkyl-substituted oxadiazole rings. On the basis of these calculations, the difference in the N 1s \rightarrow π^* transition energy between PPOD and DPOD is a combination of a core level shift (0.38 eV) and a valence shift (0.37 eV). The core level shift is due to the differing inductive effect of the phenyl versus ethyl group on the oxadiazole ring, while the valence π^*

shift is due to electronic delocalization. This is another example of why "larger" building blocks must be considered for fingerprint analysis of polymers with electronic delocalization.

The calculations presented here support our assignments of the 1st peak and 2nd shoulder in PPOD as $N\ 1s \rightarrow \pi^*$ transitions, while the 3rd peak in PPOD (at 402.5 eV) is an $N\ 1s \rightarrow \sigma^*$ transition with large s character.

The features (B) at 400.9 eV in the spectrum of Kevlar appear at approximately the same energy as peak A_2 . These features are related to delocalization of the phenyl π^* density onto the amine groups, creating an $N\ 1s \rightarrow p^*$ transition. This effect has been observed in the $N\ 1s$ spectra of phenyl-substituted urea and urethane molecules.²⁷ Here, Kevlar is a particularly good "fingerprint" model for the amine electronic environment. In AF51, there is one amine nitrogen atom and two oxadiazole nitrogen atoms; therefore, the relative amine contribution will be weak in the spectrum of AF51.

The most intense feature in the spectrum of AF51 (E) occurs at 404.5 eV and is assigned to a $N\ 1s \rightarrow \pi^*_{N=O}$ transition of the nitro group. This corresponds to the results of Turci et al. on nitrobenzene and other nitroanilines.²⁵ On its high-energy side, resonance E is superimposed with the contribution of a $N\ 1s \rightarrow \sigma^*$ transition (F) at 405.0 eV, whose σ^* character can be seen from its opposite angle dependence in relation to that of peak E in Figure 9. For energies ≥ 406 eV all spectra show further contributions of various $N\ 1s \rightarrow s^*$ transitions.

O K-Edge. The O K-edge absorption spectra were measured at photon energies between 528 and 570 eV and are shown in Figure 8. Energies and assignments of AF51 are presented in Table 5. The O K-edge spectrum of AF51 is a superposition of contributions from an oxadiazole oxygen atom, the carbonyl oxygen atom, and the two nitro group oxygen atoms. The first feature in the spectrum of AF51 is believed to be a superposition of two resonances, A and B, and has a fwhm of about 1.6 eV, which is twice as large as the fwhm of resonance B in the spectra of Kevlar and PET. Resonance A at 531.0 eV is attributed to a $O\ 1s(NO_2) \rightarrow \pi^*_{N=O}$ transition of the NO_2 functional group. Here we rely on the ISEELS measurements on nitrobenzene reported by Turci et al.²⁵ We believe that an $O\ 1s(C=O) \rightarrow \pi^*_{C=O}$ resonance (B) is superimposed with resonance A in AF51. This hypothesized contribution is expected to occur at 531.5 eV, similar to the energy of the $O\ 1s \rightarrow \pi^*_{C=O}$ resonance in Kevlar and PET.⁹ Clearly, the carbonyl electronic transitions in Kevlar and PET are expected to be somewhat affected by π^* delocalization between the phenyl group and the carbonyl group, while this delocalization will be different in AF51.

The peak (C) at 534.7 eV is attributed to a $O\ 1s \rightarrow \pi^*$ transition of the oxadiazole ring; it lies exactly at the same energy for AF51 and PPOD. Its π character can be seen from the angle-resolved spectra of AF51. The features above 537 eV (D and E) are believed to be superimposed $O\ 1s \rightarrow \sigma^*_{C-O}$, $O\ 1s \rightarrow \sigma^*_{N-O}$, $O\ 1s \rightarrow \sigma^*_{C=O}$, and $O\ 1s \rightarrow \sigma^*_{N=O}$ resonance contributions.

Linear Dichroism. Considering the angle-resolved NEXAFS spectra of an OMBD film of AF51 in Figure 9, it should be noted that the NEXAFS method is a localized spectroscopy which probes the amplitude and directionality of unoccupied molecular orbitals on atoms characterized by a core hole.⁵ Only the spatial orientation (direction of maximal orbital amplitude) of a selected orbital determines the angle dependence of K-edge absorption spectra. In this picture the π systems of the phenyl and oxadiazole rings can be represented by a " π vector" which is orthogonal to the ring plane whereas the

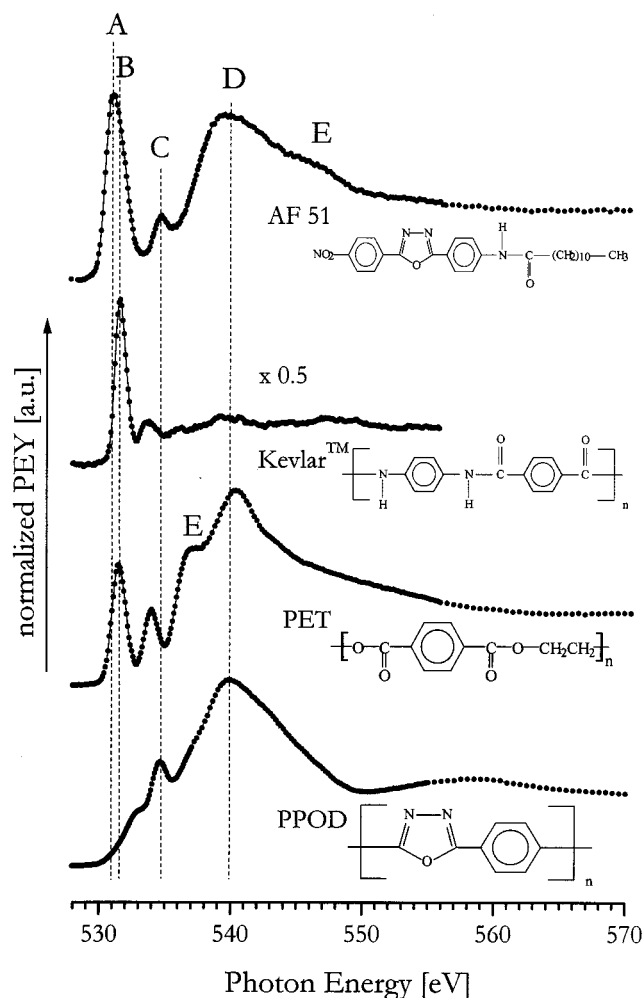


Figure 8. O K-edge X-ray absorption spectra of AF51, Kevlar, PET, and PPOD for fingerprinting. The interpretation of the spectral features marked by capitals is given in the text and in Table 5.

Table 5. Assignment of the Resonant Features for the O K-Edge NEXAFS Spectra of the Oxadiazole Molecule AF51

resonance	energy (eV)	assignments		
		oxadiazole	carbonyl	NO_2
A	531.0	π^*		$\pi^*_{N=O}$
B	531.5		$\pi^*_{O=C}$	
C	534.7	π^*		
D	540		σ^*_{O-R}	
E	546		σ^*_{O-R}	

π systems of the carbonyl and nitro groups can be represented by a " π vector" which is orthogonal to their internuclear axis.⁵ As all these π systems of AF51 are coupled by aromatic conjugation, their " π vectors" are nearly parallel. Considering the angular dependence of the π^* resonance intensities at the C, N, and O K-edges, we found that the maximum intensity for the π^* resonances of the phenyl rings, the oxadiazole ring, and the nitro and carbonyl groups is achieved at normal incidence of the linearly polarized synchrotron radiation. This means that the normal vectors of the π bonds of the above-mentioned groups preferentially lie in the surface plane. As those vectors are standing normal to the molecular axis, one can conclude for the outermost molecular layers a preferentially upright orientation of the molecular axis of the oxadiazole molecules relative to the surface plane of the film. That preferential orientation of the AF 51

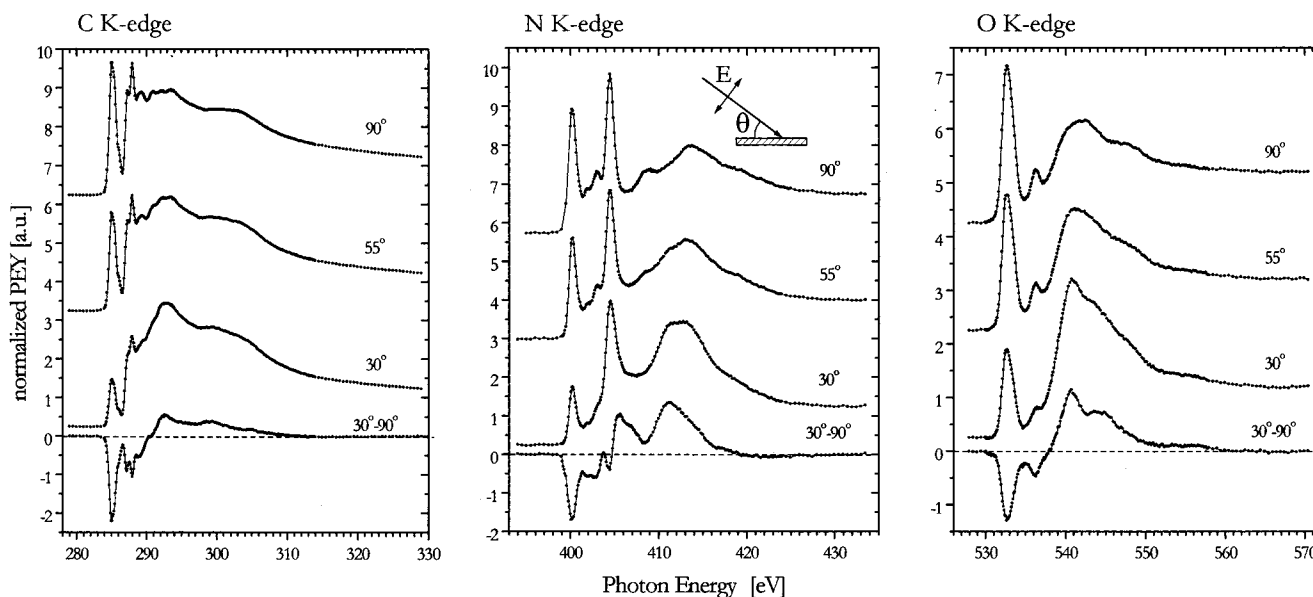


Figure 9. Angle-resolved partial electron yield C, N, and O K-edge X-ray absorption spectra of the surface of an OMBD film of AF51 oxadiazole molecules (see Figure 1). The spectra were taken at normal incidence (90°), near the magic angle (55°), and at grazing incidence. Additionally the difference spectra of the normalized and energetically aligned 90° and 30° spectra are given. The absorption geometry is illustrated in an inset to the N K-edge spectra.

molecules is consistent with the results of the X-ray reflection experiments obtained with the AF 51 films. Considering the angular dependence of the resonance intensities in the σ region of the C, N, and O K-edge spectra, we found, consequently, an opposite dependence.

Conclusions

OMBD and LB films formed by the amphiphilic substituted 2,5-diphenyl-1,3,4-oxadiazole AF51 are ordered supramolecular systems with a preferentially upright molecular orientation in the outermost layer. This preferentially upright orientation of the oxadiazole molecules found by X-ray specular reflection measurements could be proved for the surfaces of both kinds of films by adequate linear dichroism phenomena observed in the angle-resolved NEXAFS spectra.

The main resonant features in the C, N, and O K-edge NEXAFS spectra of AF51 films were attributed to corresponding functional groups by comparison to NEXAFS

spectra of substances containing the same or similar molecular moieties. Additionally, detailed quantum chemical simulations of C and N core excitation spectra were performed in order to confirm the results of the fingerprint approach mentioned above.

AF51 films prepared by the LB technique show the same spectral and orientation features in NEXAFS spectroscopy as the respective OMBD films.

Acknowledgment. We thank Dr. W. Braun and M. Mast (BESSY, Berlin) for their support and I. Koprinarov (BAM, Berlin) for his assistance during the measurements at BESSY. Special thanks are due to Mrs. A. Freydanck (IDM, Teltow) for supplying the oxadiazole molecules and Dr. T. Köpnick (IDM, Teltow) for providing several spin-coating films. This work was supported by the DFG under Grant BR 1451.

LA980888T